Cell Reports, Volume *25*

Supplemental Information

CMV Primes Functional Alternative Signaling in Adaptive ΔG NK Cells but Is Subverted by Lentivirus Infection in Rhesus Macaques

Spandan V. Shah, Cordelia Manickam, Daniel R. Ram, Kyle Kroll, Hannah Itell, Sallie R. Permar, Dan H. Barouch, Nichole R. Klatt, and R. Keith Reeves

Supplemental Figure 1

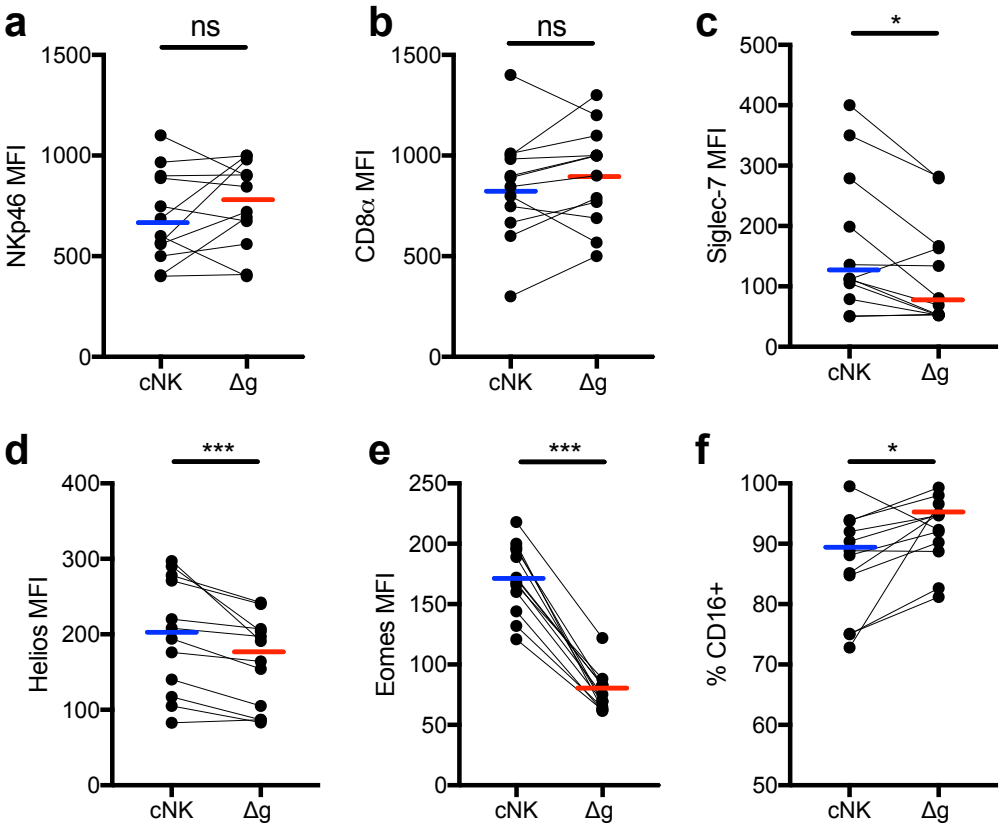

Supplemental Figure 1. Disparate marker expression on Δg NK cells, Related to Figure 1. Density of surface NKp46 (**a**), CD8α (**b**), Siglec-7 (**c**), and intracellular Helios (**d**) and Eomes (**e**) in Δg and cNK cells in PBMC from rhCMV-infected macaques. (**d**) Percentage of CD16+ subpopulations among total Δg and cNK cells. Horizontal lines indicate medians and connecting lines are shown between individual animals. Statistical evaluations were made by Wilcoxon Matched Pairs test; *, $P < 0.05$; ***, $P < 0.001$. MFI, median fluorescence intensity.

Supplemental Figure 2

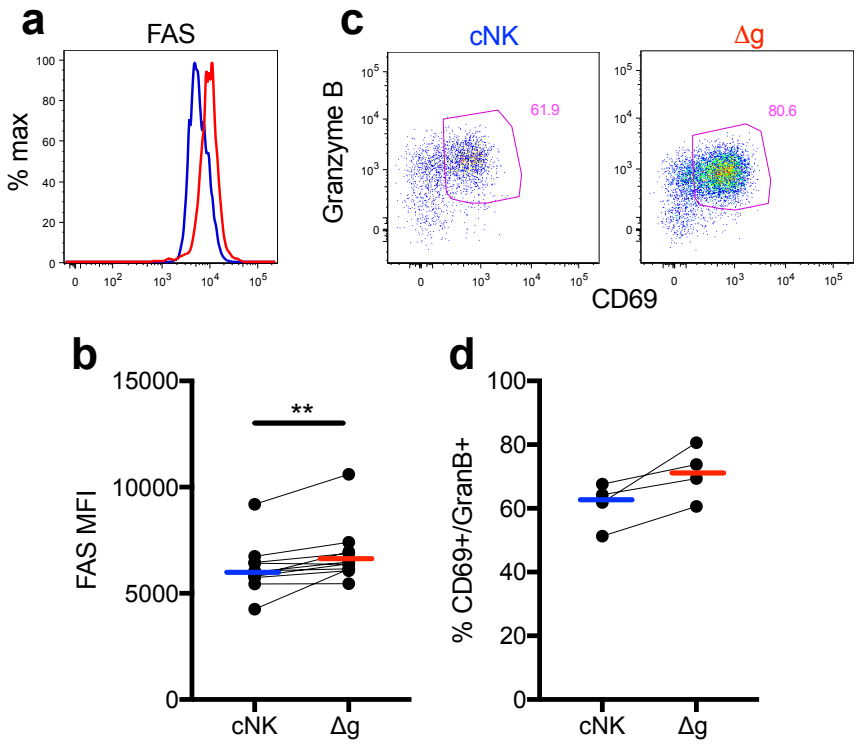

Supplemental Figure 2. Increased FAS and cytotoxic arming of Δg NK cells, Related to Figure 1. (**a**) Representative histograms and (**b**) density measurements of cell surface FAS (MFI, median fluorescence intensity) on Δg and cNK cells in PBMC from CMV+ macaques. (**c**) Representative flow cytometry plots and (**d**) percentages of cytotoxic-armed Granzyme B+/CD69+ Δg and cNK cells in PBMC from rhCMV-infected macaques. Horizontal lines indicate medians and connecting lines are shown between individual animals. Statistical evaluations were made by Wilcoxon Matched Pairs test; **, $P < 0.01$.

Supplemental Figure 3

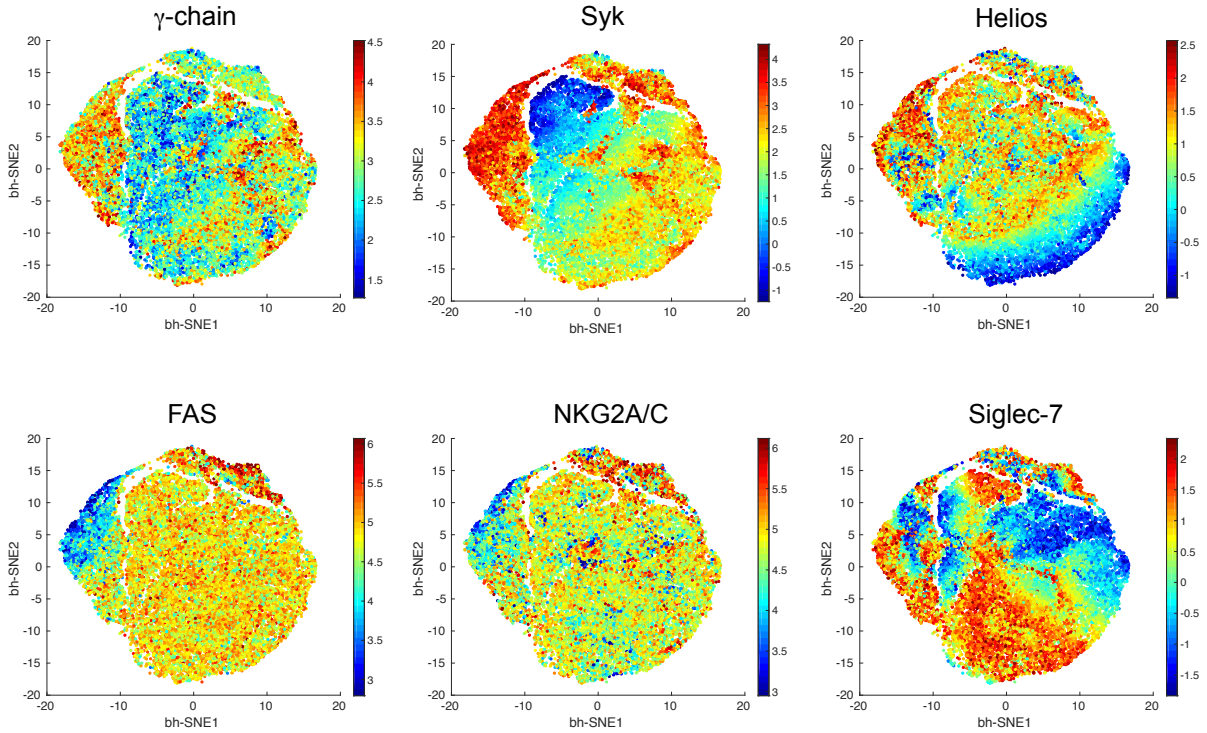

Supplemental Figure 3. Δg NK cell diversification, Related to Figure 1. Composite *t*-SNE of Δg NK cells from rhCMV-infected rhesus macaques as shown in **Fig. 1d**; individual markers are indicated. Data points represent individual cells and colors depict intensity of protein expression.

.

Supplemental Figure 4

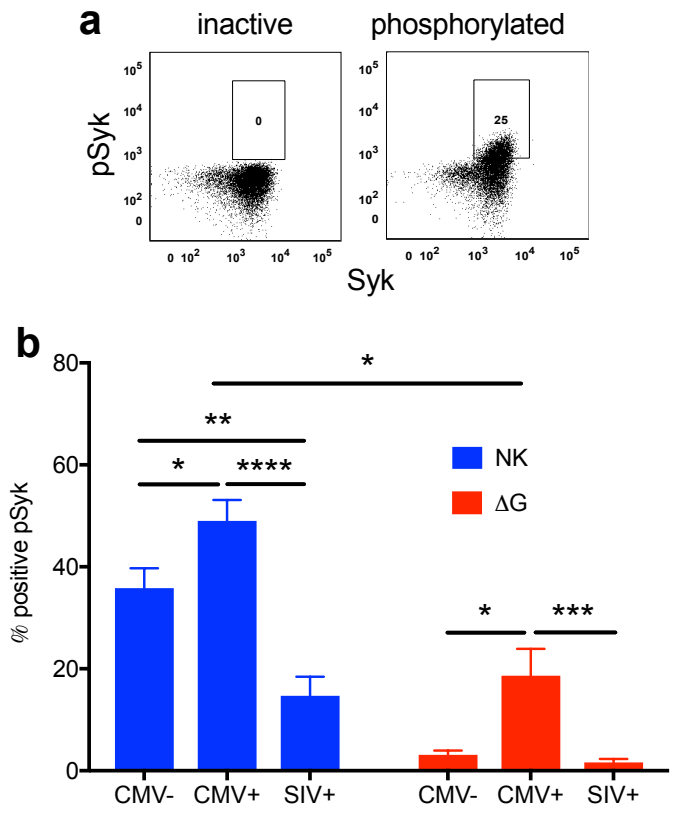

Supplemental Figure 4. Syk is inactive in Δg NK cells, Related to Figure 6. Representative plots from inactive and activated (**a**) phosphoSyk samples are shown. Δg and cNK cells were gated as shown in Figure 1. (**b**) Bars represent means ± SEM of 6-10 animal samples per group. Statistical comparisons between infection groups were conducted by Mann-Whitney *U* test, and statistical comparisons between conditions for individual animals were conducted using Wilcoxon-Matched pairs test; *, $P < 0.05$; **, $P < 0.01$; ***, $P < 0.001$, ****, $P < 0.0001$.

Supplemental Figure 5

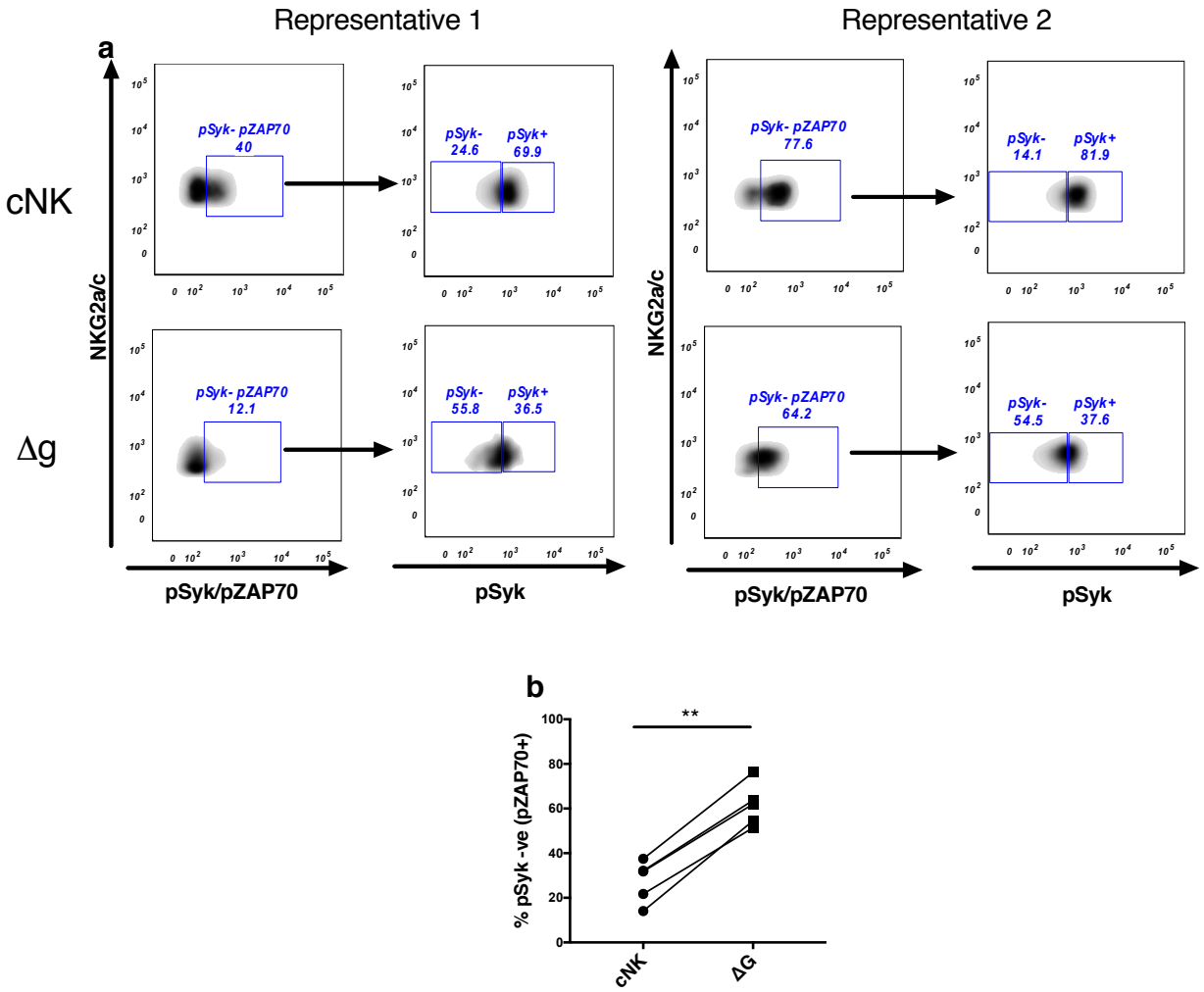

Supplemental Figure 5. Active ZAP70 is elevated in Δg NK cells, Related to Figure 6. (**a**) Representative gating strategy to identify pZAP70 in Δg and cNK cells. Since a fully specific pZAP70 antibody does not exist, frequencies of pSyk+ cells were subtracted from a dual pSyk/pZAP70-specific antibody to determine frequencies of pZAP70 expression. (**b**) Data are shown for percentages of pSyk- Δg and cNK cells between individual rhCMV-infected animals. Statistical comparisons were conducted using Wilcoxon-Matched pairs test; **, $P < 0.01$.

Supplemental Figure 6

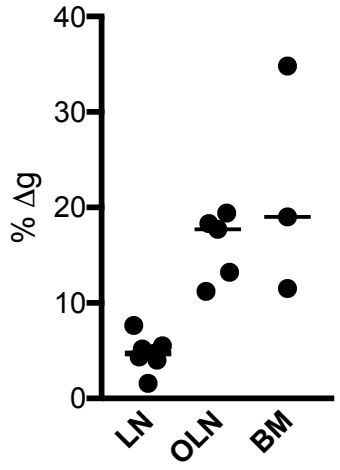

Supplemental Figure 6. Δg NK cells in LN, OLN and bone marrow, Related to Figure 3. Frequencies among bulk NK cells in rhCMV-infected, but otherwise normal rhesus macaques. Bars indicate medians. LN, lymph nodes; OLN, oral lymph nodes.